High-Order Finite Element for the resolution of time-harmonic Maxwell equations

Marc Duruflé
INRIA Rocquencourt

Model Problem

$$
\begin{aligned}
-\mathrm{i}\omega\, \varepsilon(x)\, \vec{E}(x) \;-\; \mathrm{curl}\, \vec{H}(x) &= 0 && x \in \Omega \\
-\mathrm{i}\omega\, \mu(x)\, \vec{H}(x) \;+\; \mathrm{curl}\, \vec{E}(x) &= 0 && x \in \Omega \\
\nu \times \vec{E}(x) &= 0 && x \in \Gamma \\
(\nabla \times \vec{E}) \times \nu &= \mathrm{i}k\, (\nu \times \vec{E}) \times \nu + \\
& \quad (\nabla \times \vec{E}^i) \times \nu \;-\; \mathrm{i}k\, (\nu \times \vec{E}^i) \times \nu && x \in \Sigma
\end{aligned}
\qquad (1)
$$

$\vec{E}^i \;=\; \vec{E}^0\, exp(\mathrm{i}\vec{k}\, \vec{x})$: incident plane wave

$\vec{E}^0$ the polarisation of the plane wave

A digression : the transparency condition

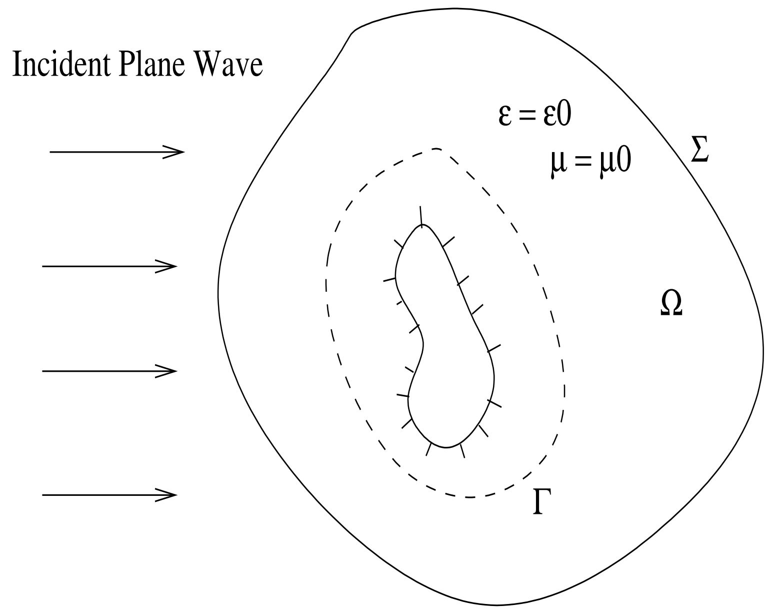

Homogeneous media between an exterior boundary Σ and an interior boundary Γ.

Modification of the first-order absorbing boundary condition

$$\begin{aligned}\frac{\partial u}{\partial \nu(x)}(x) - \mathrm{i}k u(x) &= \int_\Gamma \left(\frac{\partial^2 \phi(x,y)}{\partial \nu(x) \partial \nu(y)} - \mathrm{i}k \frac{\partial \phi(x,y)}{\partial \nu(y)} \right) u(y) \\ &- \left(\frac{\partial \phi(x,y)}{\partial \nu(x)} - \mathrm{i}k \phi(x,y) \right) \frac{\partial u}{\partial \nu(y)} dy \quad x \in \Sigma\end{aligned}$$

Outline of the presentation

- Edge finite element on quadrilaterals, first and second Nedelec's family

- Discontinuous Galerkin method on quadrilaterals

- Scattering by a diedra disk

- Comparison with edge finite elements on triangles

- 3-D examples

A first approach : discretization of the H(curl) space

Variational formulation of second order in $\vec{E}$

$$-k^2 \int_\Omega \varepsilon_r \vec{E} \cdot \vec{\varphi} + \int_\Omega \frac{1}{\mu_r} (\nabla \times \vec{E}) \cdot (\nabla \times \vec{\varphi}) - ik \int_\Sigma (\nu \times \vec{E}) \cdot (\nu \times \vec{\varphi}) = \int_\Sigma \vec{g} \cdot \vec{\varphi} \quad (2)$$

$$\vec{E}, \vec{\varphi} \in \mathrm{H(curl,}\Omega) = \{\vec{u} \in \left(L^2(\Omega)\right)^2 \text{ and } \nabla \times \vec{u} \in L^2(\Omega)\}$$

Question : How can this space be discretized ?

Part One : Nedelec's first family on quadrilaterals

Space of approximation

$$V_h = \{ \vec{u} \in \ \mathrm{H(curl,}\Omega) \ \text{so that } DF_i^t \, \vec{u} \circ F_i \in Q_{r-1,r} \times Q_{r,r-1} \} \tag{3}$$

Basis functions

$$\begin{aligned} \vec{\hat{\varphi}}^1_{i,j}(\hat{x},\hat{y}) &= \hat{\psi}^G_i(\hat{x}) \, \hat{\psi}^{GL}_j(\hat{y}) \, \vec{e}_x \quad 1 \leq i \leq r \quad 1 \leq j \leq r+1 \\ \vec{\hat{\varphi}}^2_{j,i}(\hat{x},\hat{y}) &= \hat{\psi}^{GL}_j(\hat{x}) \, \hat{\psi}^G_i(\hat{y}) \, \vec{e}_y \quad 1 \leq i \leq r \quad 1 \leq j \leq r+1 \end{aligned} \tag{4}$$

ψ_i^G, ψ_i^{GL} lagrangian functions linked with respectively Gauss and Gauss-Lobatto points.

Degrees of freedom and quadrature

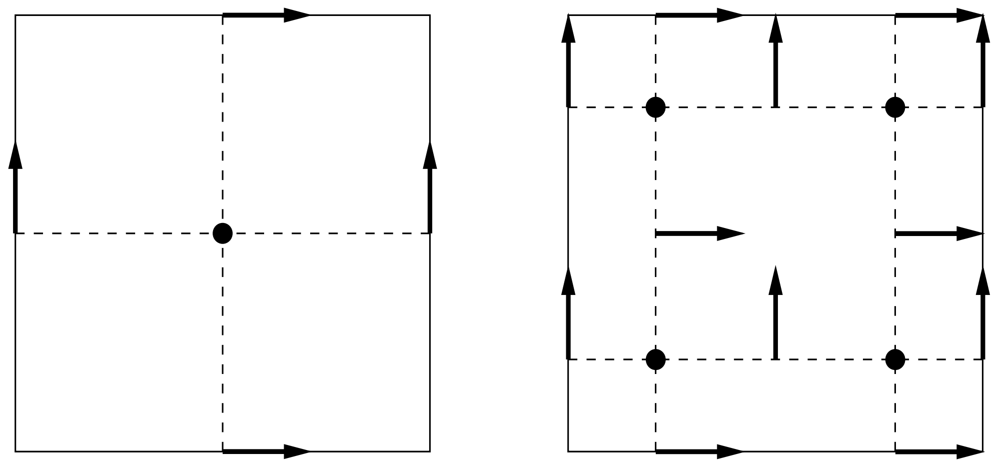

$r = 1$ on left $\quad r = 2$ on right

The arrows give the position of degrees of freedom.

No mass lumping for this family, the mass matrix is big !

Gauss points to integrate the stiffness matrix.

Gauss-Lobatto points to integrate the mass matrix

$\Rightarrow$ Discrete factorization of these two matrices

$\Rightarrow$ Huge gain of storage and gain of time

Discrete Factorization for the Nedelec's first family on quadrilaterals

Mass matrix

$$\begin{aligned} M_{a,b} &= \int_{\hat{K}} |J_i| \, DF_i^{-1} \, \varepsilon_r \, DF_i^{-t} \, \vec{\hat{\phi}}_a \cdot \vec{\hat{\phi}}_b \, d\hat{x} \, d\hat{y} \\ \vec{\hat{\phi}}_a &= \hat{\psi}_i^G(\hat{x}) \, \hat{\psi}_j^{GL}(\hat{y}) \, \vec{e}_x \\ \vec{\hat{\phi}}_b &= \hat{\psi}_l^{GL}(\hat{x}) \, \hat{\psi}_k^G(\hat{y}) \, \vec{e}_y \end{aligned}$$

$\hat{\psi}_i^G$ lagrangian function linked with the Gauss point i

Integration using Gauss-Lobatto quadrature points

$$Mh_{a,b} = \sum_{m,n} (B_{21}\omega)_{m,n} \hat{\psi}_i^G(\xi_m^{GL}) \, \hat{\psi}_j^{GL}(\xi_n^{GL}) \, \hat{\psi}_l^{GL}(\xi_m^{GL}) \, \hat{\psi}_k^G(\xi_n^{GL})$$

En ayant noté $B = |J_i| \, DF_i^{-1} \, \varepsilon_r \, DF_i^{-t}$

Discrete Factorisation

This coefficient of the mass matrix is reduced to

$$\int_{K_i} \varepsilon_r \vec{\phi}_a \cdot \vec{\phi}_b = (B_{21}\omega)_{l,j} \hat{\psi}_i^G(\xi_l^{GL}) \hat{\psi}_k^G(\xi_j^{GL}) \tag{5}$$

The matrix-vector product $M_h^{21} E = X$ is written

$$X_{l,k}^2 = \sum_{i,j} (B_{21}\omega)_{l,j} \hat{\psi}_i^G(\xi_l^{GL}) \hat{\psi}_k^G(\xi_j^{GL}) E_{i,j}^1 \tag{6}$$

We can separate the product in two steps

$$\begin{aligned} v_{l,j}^1 &= \sum_i \hat{\psi}_i^G(\xi_l^{GL}) E_{i,j}^1 \\ X_{l,k}^2 &= \sum_j (B_{21}\omega)_{l,j} \hat{\psi}_k^G(\xi_j^{GL}) v_{l,j}^1 \end{aligned} \tag{7}$$

Advantages of this factorization

- Storage of the matrix $|J_i|\, DF_i^{-1}\, \varepsilon_r\, DF_i^{-t}$ on Gauss-Lobatto points

- Storage of the scalar $\dfrac{1}{\mu_r J_i}$ on Gauss points
  $\Rightarrow$ Gain in storage

- Cost of the matrix-vector product $O(r^3)$ r begin the order of approximation
  $\Rightarrow$ Gain in time computation

Study of the scattering of a perfectly conducting disk

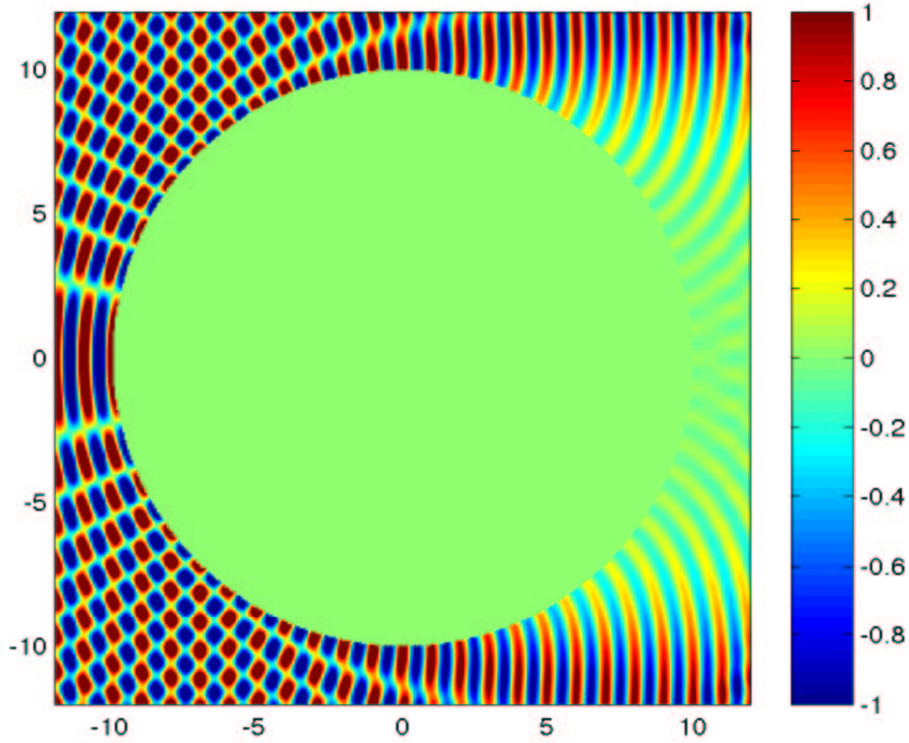

Real part of the curl of the total field (in truth H), the wave comes from left to right. The radius of the disk is 10 m, the frequence is 300 Mhz, transverse Electric case. Analytical solution.

Some notations

N = nombre de degré de libertés total

R = 12 m, radius of the outside boundary

r = 10 m, radius of the inside boundary

Area = $\pi(R^2 - r^2)$ number of square wavelength in the computational domain

$$h = \sqrt{\frac{2 * Area}{N}}$$ **space step**

Convergence on triangular meshes split

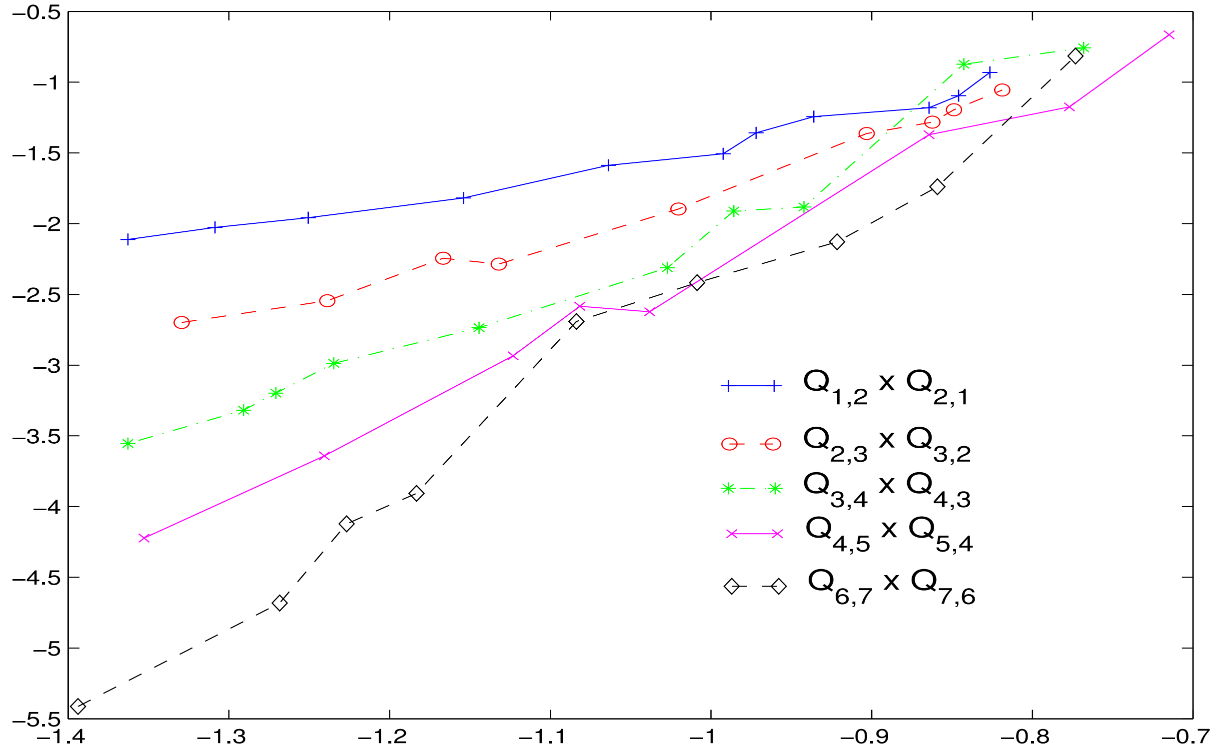

H(curl) error according to the space step in log-log scale, between the numerical solution and the analytical one. Experiences in the case of the disk, with a transparency condition and curved finite elements.

Nedelec's second family for quadrilaterals

Space of approximation

$$V_h = \{ \vec{u} \in \ \mathrm{H(curl,}\Omega) \text{ such as } DF_i^t \, \vec{u} \circ F_i \in (Q_r)^2 \} \tag{8}$$

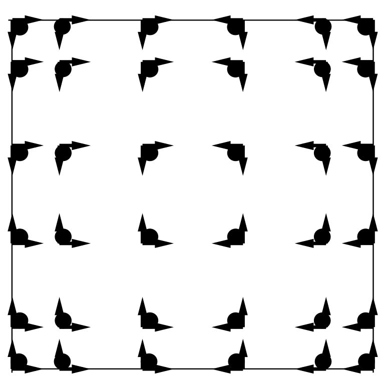

$\xi_k, \ k = 1..(r+1)$

are the Gauss-Lobatto quadrature points

Degrees of freedom for E

$\Rightarrow$ Scalar Lagrange basis functions : $\psi_{\ell,m} \circ F_i \ = \ \hat{\psi}_{\ell,m}$

$$\hat{\psi}_{\ell,m}(\hat{x},\hat{y}) \ = \ \prod_{i=1\, i\neq\ell}^{r+1} \frac{\hat{x} - \xi_\ell}{\xi_i - \xi_\ell} \prod_{j=1\, j\neq m}^{r+1} \frac{\hat{y} - \xi_m}{\xi_j - \xi_m} \tag{9}$$

$\varphi_i \ = \ \psi_i \vec{e_x} \text{ ou } \psi_i \vec{e_y}$ vectorial basis functions

Properties of matrices

Mass matrix $B_h = \int_{\hat{K}} J_i \, DF_i^{-1} \varepsilon_r DF_i^{-t} \vec{\hat{\varphi}}_j \cdot \vec{\hat{\varphi}}_k$ block-diagonal

Stiffness matrix $K_h = \int_{\hat{K}} \frac{1}{J_i} \frac{1}{\mu_r} \nabla \times \vec{\hat{\varphi}}_j \cdot \nabla \times \vec{\hat{\varphi}}_k$

Factorization of the stiffness matrix : $K_h = R_h^t D_h^{-1} R_h$

$D_h = \int_{\hat{K}} J_i \, \hat{\psi}_i \, \hat{\psi}_j$ diagonal

$R_h = \int_{\hat{K}} \hat{\psi}_i \, \nabla \times \hat{\varphi}_j$ independent of the geometry

$\Rightarrow$ Huge gain of storage and gain in time (R_h elementary sparse)

The unwanted oscillations

Presence of “spurious modes” on strongly modified meshes

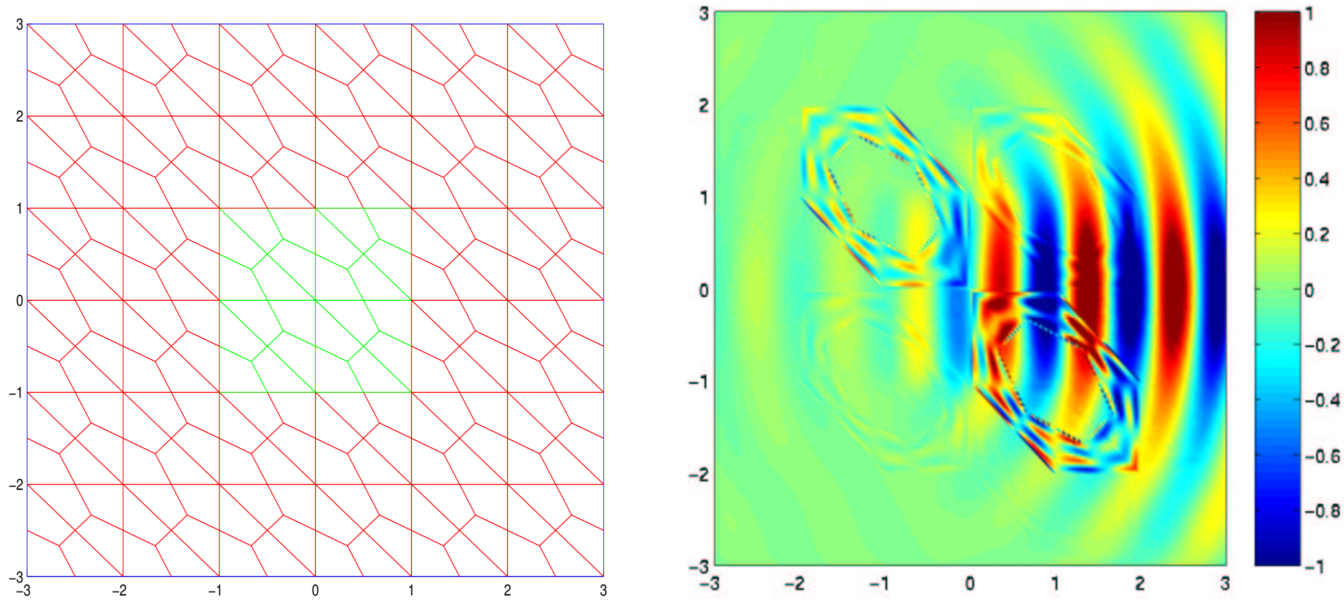

Scattering of a dielectric square. Left, mesh used for the simulations . Right, numerical solution with Q5 finite edge elements with mass-lumping.

Consequence : an erratic convergence

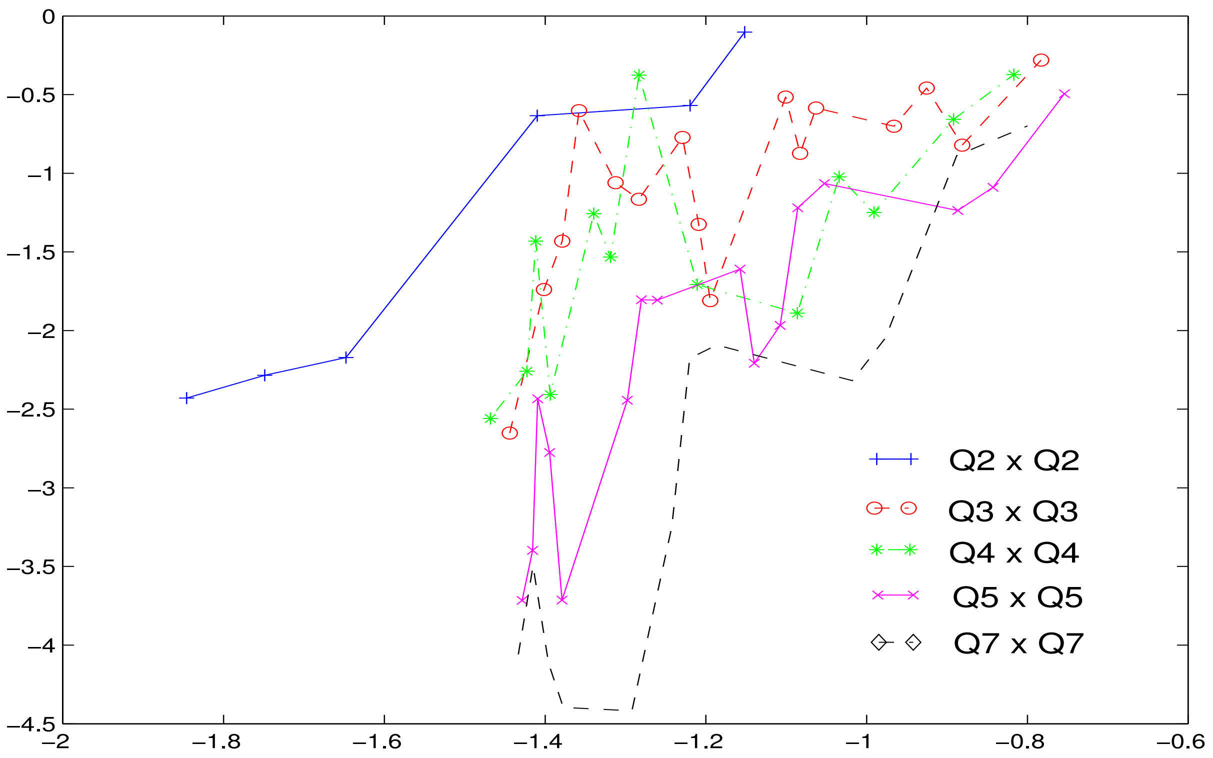

H(curl) error according to the space step in logarithmic scale, between the numerical solution and the analytical one. The meshes used for the simulations are triangular meshes split in quadrilaterals.

Nedelec's first family on triangles

$$\begin{aligned} \tilde{P}_k &= \{ \text{ homogeneous polynoms of total degree exactly } k \} \\ S_k &= \{ \vec{u} \in (\tilde{P}_k)^2 \text{ so that } \vec{x} \cdot \vec{u} = 0 \} \quad R_k = (P_{k-1})^2 \oplus S_k \end{aligned} \tag{10}$$

Space of approximation

$$V_h = \{ \vec{u} \in \text{ H-curl}(\Omega) \text{ so that } DF_i^t \, \vec{u} \circ F_i \in R_k \} \tag{11}$$

Use of interpolatory basis functions as described in

Higher Order Interpolatory Vector Bases for Computational Electromagnetics

R. D. Graglia, D. R. Wilton, A. F. Peterson

Nedelec's second family on triangles

Space of approximation

$$V_h = \{\vec{u} \in \text{H-curl}(\Omega) \text{ so that } DF_i^t\,\vec{u} \circ F_i \in (P_r)^2\} \tag{12}$$

Use of hierarchic basis as described in

Higher-Order Finite Element Methods

P. Solin, K. Segeth, I. Dolezel

A first comparison on the convergence

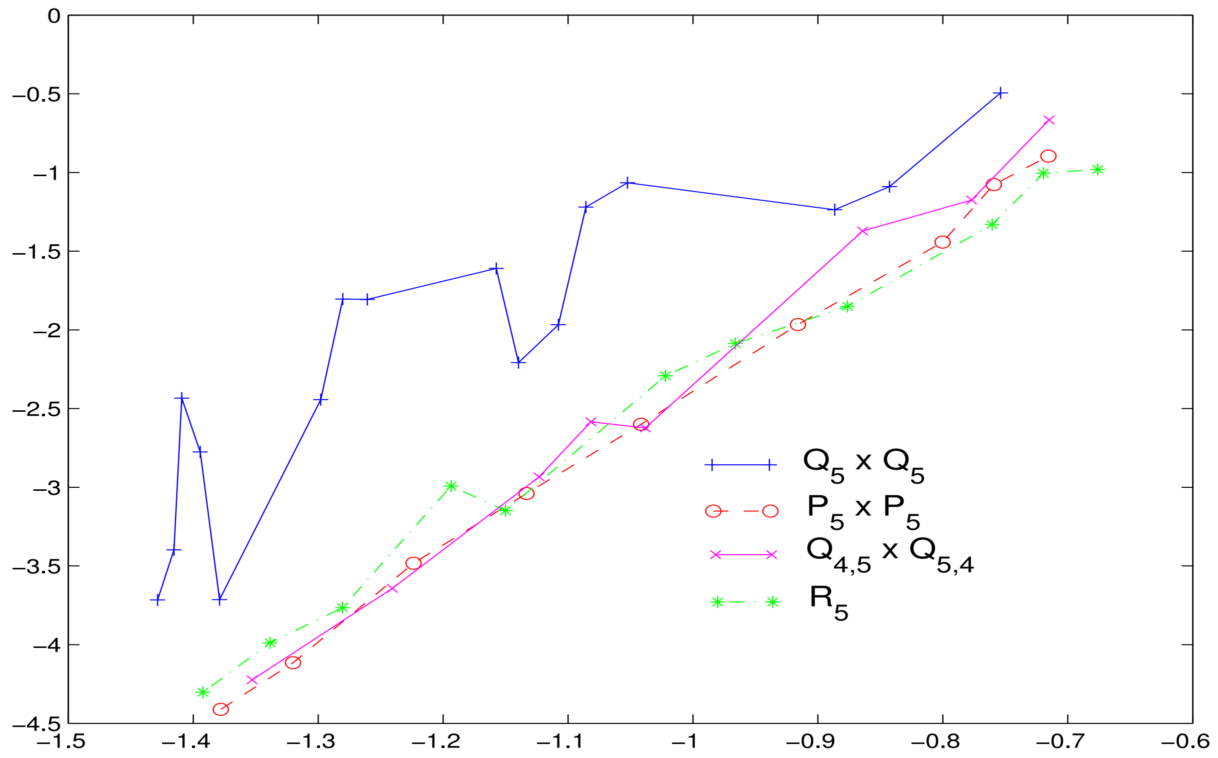

Error H(curl) according to the space step in logarithmic scale, between the numerical solution and the analytical one. The same order of approximation 5 is used.

Part Two : Discontinuous Galerkin method on quadrilaterals

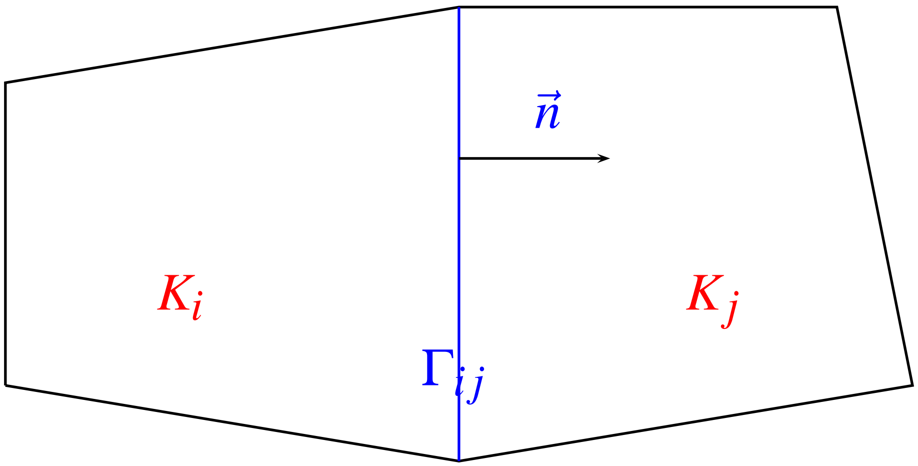

Let us notice that

$$\begin{aligned} \{H\} &= \frac{1}{2}(H_i + H_j) \\ [\,\vec{E}] &= (\vec{E}_i - \vec{E}_j) \end{aligned} \tag{13}$$

Discontinuous Galerkin variational formulation

System in $\vec{E}$ and H

$$\begin{aligned} -k^2 \int_{K_i} \varepsilon_r \vec{E} \cdot \vec{\varphi} \;\; - \int_{K_i} H \, \nabla \times \vec{\varphi} \;\; - \int_{\partial K_i} \{H\} \, \vec{\varphi} \times \vec{\nu} &= 0 \\ - \int_{K_i} \mu_r H \, \psi \;\; - \int_{K_i} \nabla \times \vec{E} \, \psi \;\; - \frac{1}{2} \int_{\partial K_i} [\vec{E}] \times \vec{\nu} \, \psi &= 0 \end{aligned} \tag{14}$$

+ Boundary integrals coming from the Silver-Müller condition

$$\begin{aligned} & -\frac{\mathrm{i}k}{2} \int_{\Sigma} (\vec{E} \times \vec{\nu}) \cdot (\vec{\varphi} \times \vec{\nu}) \\ & -\frac{\mathrm{i}}{2k} \int_{\Sigma} H \, \psi \end{aligned} \tag{15}$$

Approximation spaces and basis functions

$$V_h = \{ (\vec{u}, v) \in \ (L^2)^2 \times L^2 \ \text{so that } DF_i^t \, \vec{u} \circ F_i \in (Q_r)^2 \text{ and } v \circ F_i \in (Q_r) \} \qquad (16)$$

$\vec{\hat{\varphi}}_{k,l} = \hat{\psi}_k \hat{\psi}_l \, \vec{e}_x$ ou $\vec{e}_y$ basis functions for $\vec{E}$

$\hat{\psi}_{k,l} = \hat{\psi}_k \hat{\psi}_l$ basis functions for H

$\hat{\psi}_i$ Lagrangian functions linked with the Gauss-Lobatto or Gauss points

Mass-lumping if quadrature formulas of Gauss-Lobatto or Gauss are used.

Properties of mass and stiffness matrix

Block-diagonal and diagonal mass matrices

$$\begin{aligned}\int_{K_i} \varepsilon_r \vec{\varphi}_{j,k} \cdot \vec{\varphi}_{l,m} &= \omega_{j,k} J_i DF_i^{-1} \varepsilon_r DF_i^{-t} \hat{\vec{\varphi}}_{j,k} \cdot \hat{\vec{\varphi}}_{l,m} \delta_{j,l} \delta_{k,m} \\ \int_{K_i} \mu_r \psi_{j,k} \cdot \psi_{l,m} &= \omega_{j,k} J_i \mu_r \hat{\psi}_{j,k} \hat{\psi}_{l,m} \delta_{j,l} \delta_{k,m}\end{aligned} \tag{17}$$

Stiffness matrices and jump matrices independent of the geometry

$$\int_{K_i} \psi_{j,k} \nabla \times \vec{\varphi}_{l,m} = \int_{\hat{K}} \hat{\psi}_{j,k} \hat{\nabla} \times \hat{\vec{\varphi}}_{l,m} \tag{18}$$

$\Rightarrow$ Huge gain of storage and gain in time

Is the matrix symmetric ?

$\Rightarrow$ stiffness matrices transposed each other

- boundaries terms on K_i

$$-\frac{1}{2}\int H_i \phi_i \times \nu \quad -\frac{1}{2}\int H_j \phi_i \times \nu$$

$$-\frac{1}{2}\int \psi_i E_i \times \nu \quad +\frac{1}{2}\int \psi_i E_j \times \nu$$

- boundaries terms on K_j

$$+\frac{1}{2}\int H_j \phi_j \times \nu \quad +\frac{1}{2}\int H_i \phi_j \times \nu$$

$$+\frac{1}{2}\int \psi_j E_j \times \nu \quad -\frac{1}{2}\int \psi_j E_i \times \nu$$

Boundaries terms transposed each other

Comparison with finite edge elements

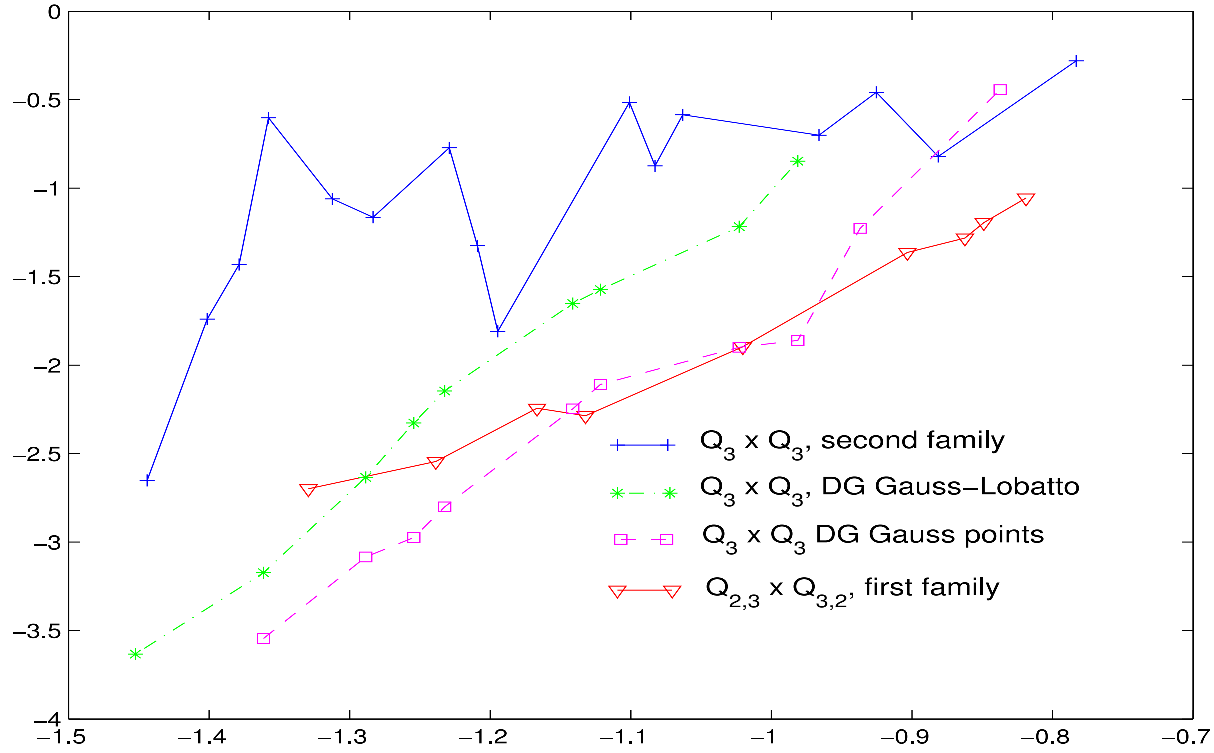

Comparison of the different quadrilateral finite elements. An order 3 has been choosen in order to make better the difference between the DG Gauss-Lobatto method and Gauss.

Comparison of the cost matrix-vector product

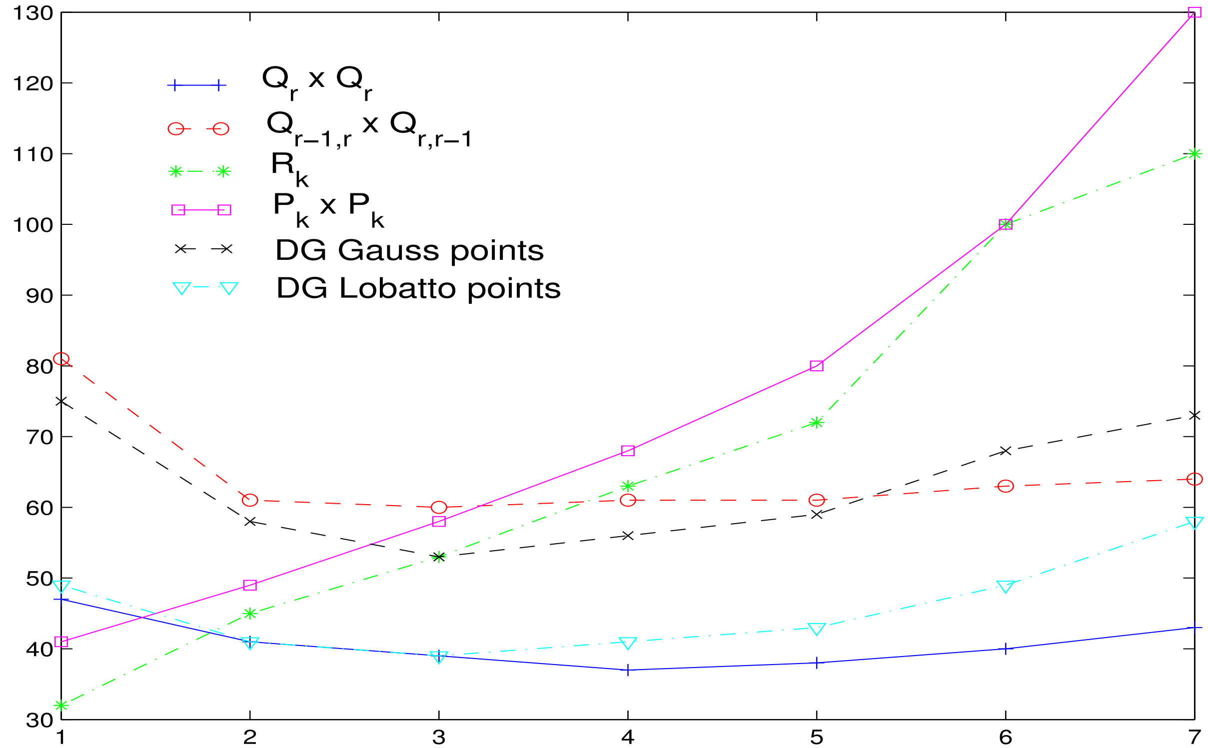

Cost of the matrix-vector product according to the order of approximation with equal number of degrees of freedom (100 000)

$\Rightarrow$ increasing cost for the triangular elements

$\Rightarrow$ quasi-constant cost for the quadrangular elements

Part Three : Scattering of a diedra-disk

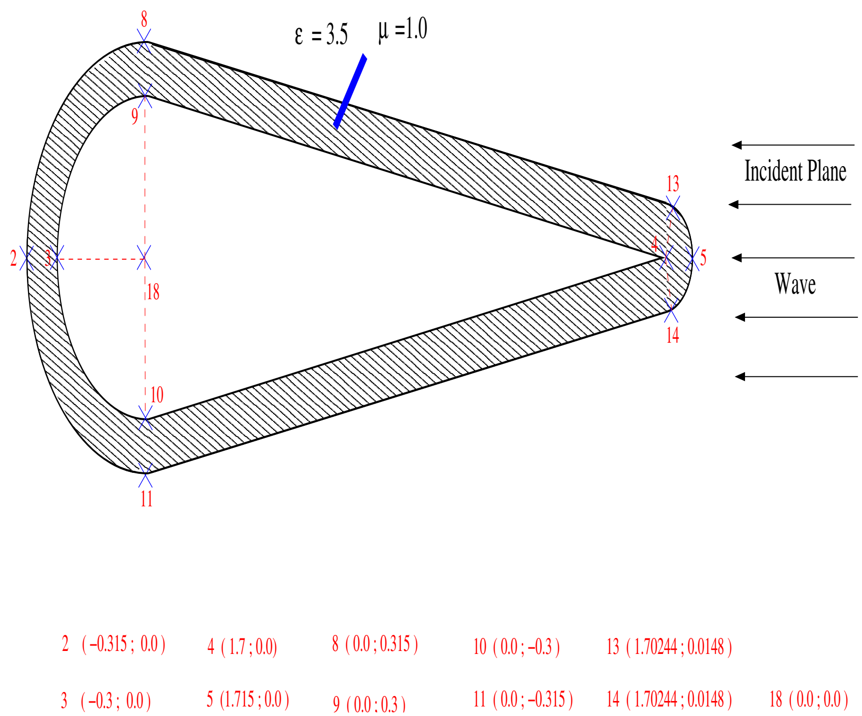

Scattering of a circular object with a conic end, by an incident plane wave. The object is coated by a thin layer of a dielectric media. The object is attacked by the pointed tip.

Transverse Electric Case (TE)

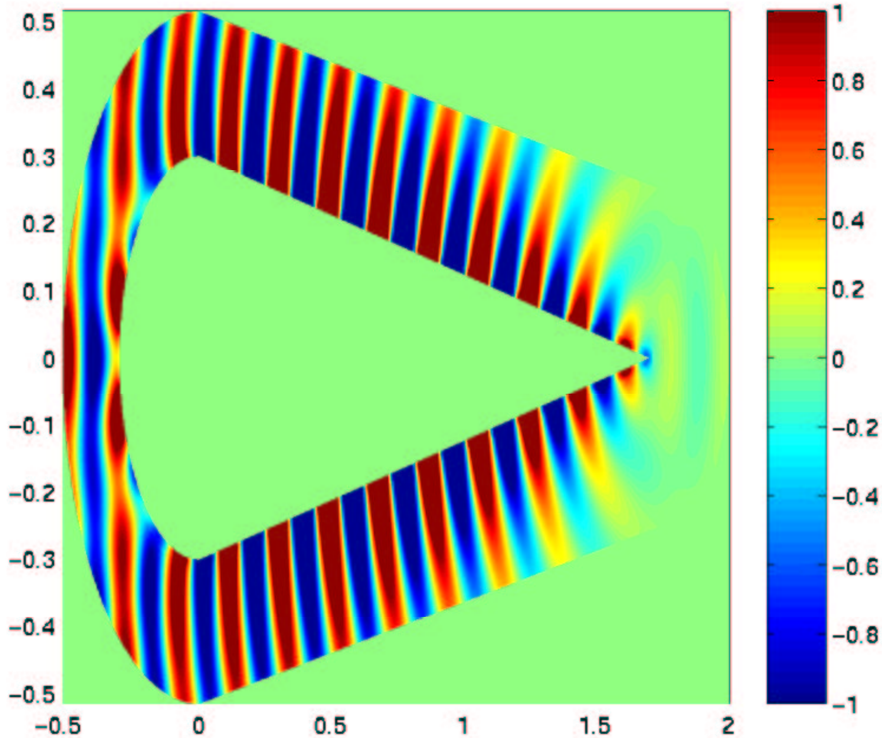

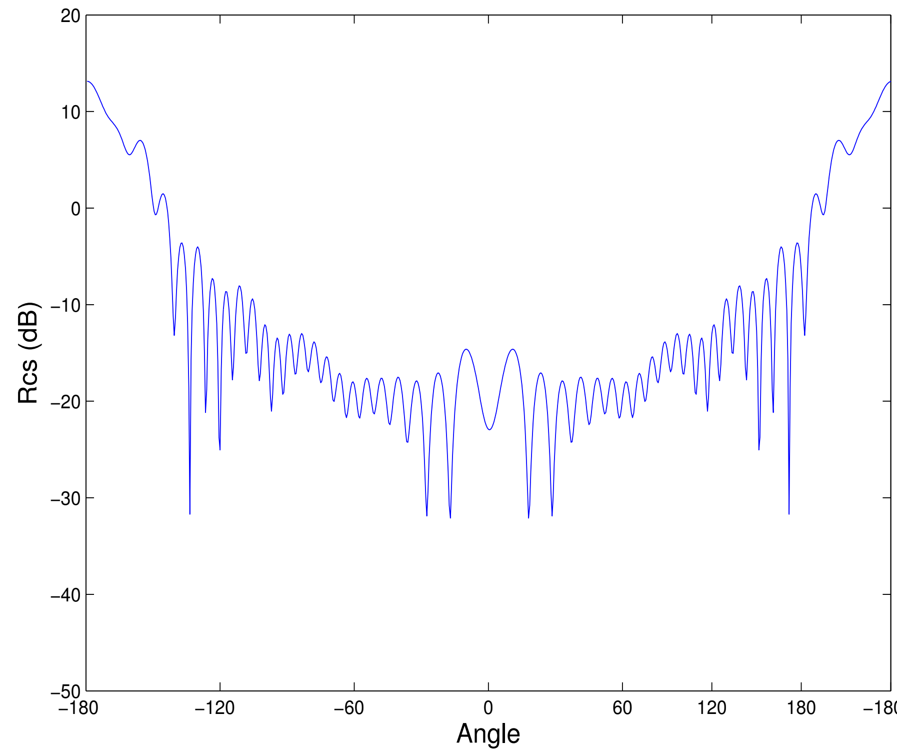

Left : Real part of the diffracted field (component z of H) in the TE case for a frequency of 1.5 Ghz

Right : RCS (Radar Cross Section) for 1.5 Ghz in the TE case

A high-frequency TM case

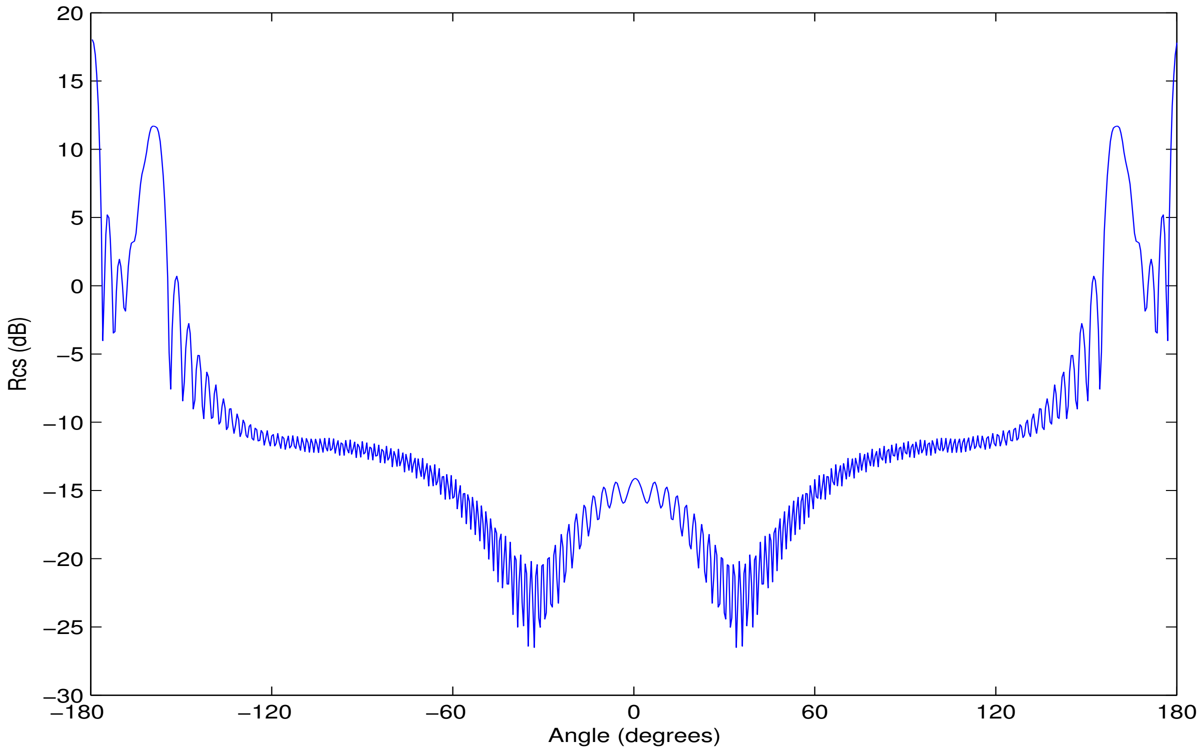

RCS for 7.5 Ghz in the TM case

Example of furtivity. Monostatic RCS is low

Our aim : compare finite elements at equal error

Comparison with an error level fixed at 1 dB

Finite element	Memory used by a direct solver	Condition number	Memory used for an iterative matrix
$Q_{3,4}$	$334Mo$	$4.3e5$	$6Mo$
R_4	$284Mo$	$4.74e6$	$52Mo$
Q_4	$443Mo$	$1.28e8$	$6.6Mo$
P_4	$260Mo$	$2.1e7$	$49Mo$

Huge gain of storage for the iterative matrix

Static condensation of inside degrees of freedom

$$A = \begin{bmatrix} A_{11} & A_{12} \\ A_{21} & A_{22} \end{bmatrix} \text{ is replaced by its Schur complement } \tilde{A} = A_{11} - A_{12}A_{22}^{-1}A_{21}$$

Preconditioner used : ILUT($1e-2$) sur $-k^2\,(1+\mathrm{i})+\vec{\Delta}$

Finite element	Memory used by a direct solver	Condition number	Memory used to precondition	Number of iterations	Time used to solve
$Q_{3,4}$	$85\,Mo$	$8.7e3$	$79\,Mo$	1000	$166s$
R_4	$111\,Mo$	$2.72e4$	$99\,Mo$	1000	$226s$
Q_4	$130\,Mo$	$2.77e6$	$118\,Mo$	NC	∞
P_4	$96\,Mo$	$1.3e4$	$56\,Mo$	1000	$143s$

Conclusion on the 2-D

- The second family on the quadrilaterals is not robust on meshes of poor quality
- The first family on the quadrilaterals is particularly efficient, even on split triangular meshes.
- Discontinuous Galerkin method has to be developped.
- Necessity of a good preconditioner

Nedelec's first family on hexahedra

Space of approximation

$$V_h = \{\vec{u} \in \mathrm{H(curl,}\Omega) \text{ so that } DF_i^t\,\vec{u} \circ F_i \in Q_{r-1,r,r} \times Q_{r,r-1,r} \times Q_{r,r,r-1}\} \quad (19)$$

Basis functions

$$\begin{aligned}
\vec{\varphi}^1_{i,j,k}(\hat{x},\hat{y},\hat{z}) &= \hat{\psi}_i^G(\hat{x})\,\hat{\psi}_j^{GL}(\hat{y})\,\hat{\psi}_k^{GL}(\hat{z})\,\vec{e}_x \quad 1 \le i \le r \quad 1 \le j \le r+1 \quad 1 \le k \le r+1 \\
\vec{\varphi}^2_{j,i,k}(\hat{x},\hat{y},\hat{z}) &= \hat{\psi}_j^{GL}(\hat{x})\,\hat{\psi}_i^G(\hat{y})\,\hat{\psi}_k^{GL}(\hat{z})\,\vec{e}_y \quad 1 \le i \le r \quad 1 \le j \le r+1 \quad 1 \le k \le r+1 \\
\vec{\varphi}^3_{k,j,i}(\hat{x},\hat{y},\hat{z}) &= \hat{\psi}_k^{GL}(\hat{x})\,\hat{\psi}_j^{GL}(\hat{y})\,\hat{\psi}_i^G(\hat{x})\,\vec{e}_z \quad 1 \le i \le r \quad 1 \le j \le r+1 \quad 1 \le k \le r+1
\end{aligned} \quad (20)$$

ψ_i^G, ψ_i^{GL} lagragian functions linked respectively with Gauss points and Gauss-Lobatto points.

Dipole

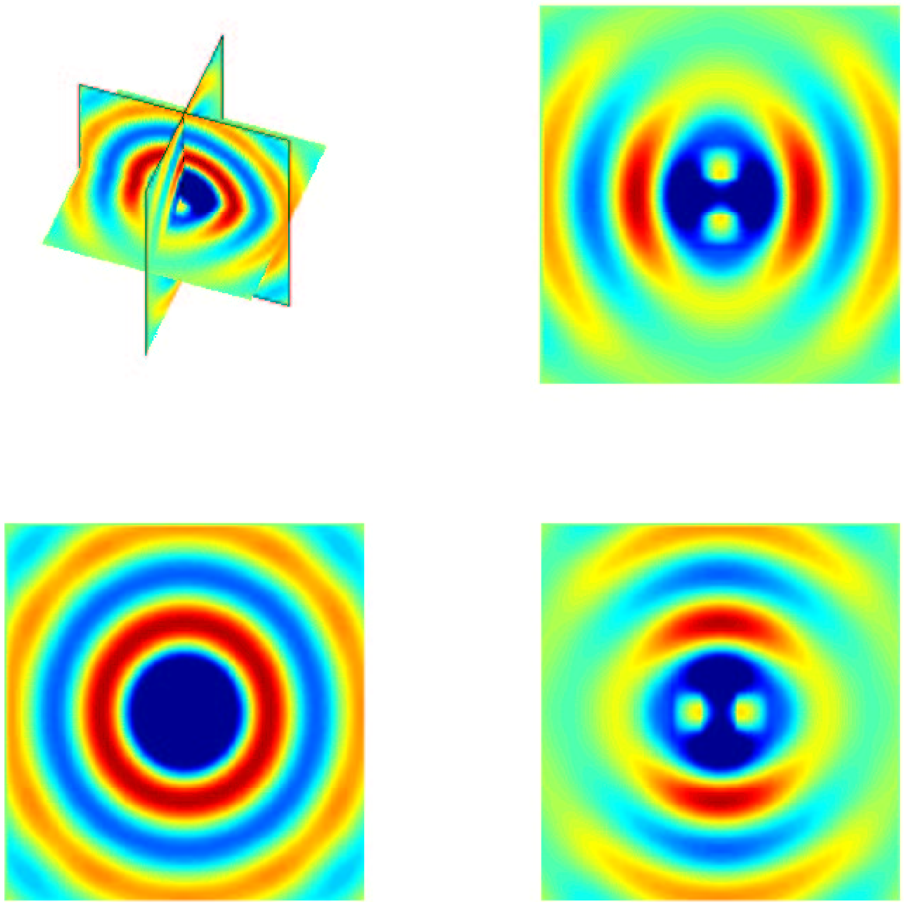

Gaussian around the origin oriented by e_x. Radius of the gaussian $0.6m$. Frequency of 300 Mhz

Real part of the component x of electric field

Diffraction by a sphere

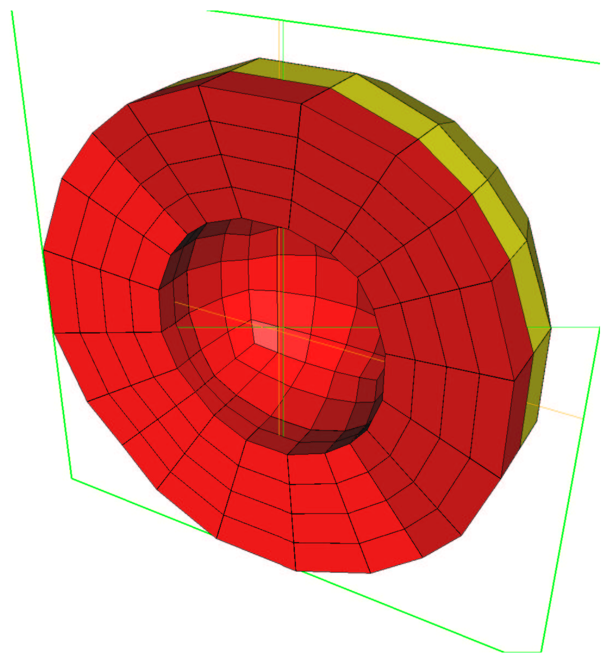

Mesh used for the numerical simulations.

Diffraction by a perfectly conducting sphere of radius 1m

plane wave $E^{inc} = exp(ikz)\, e_x$

Numerical results

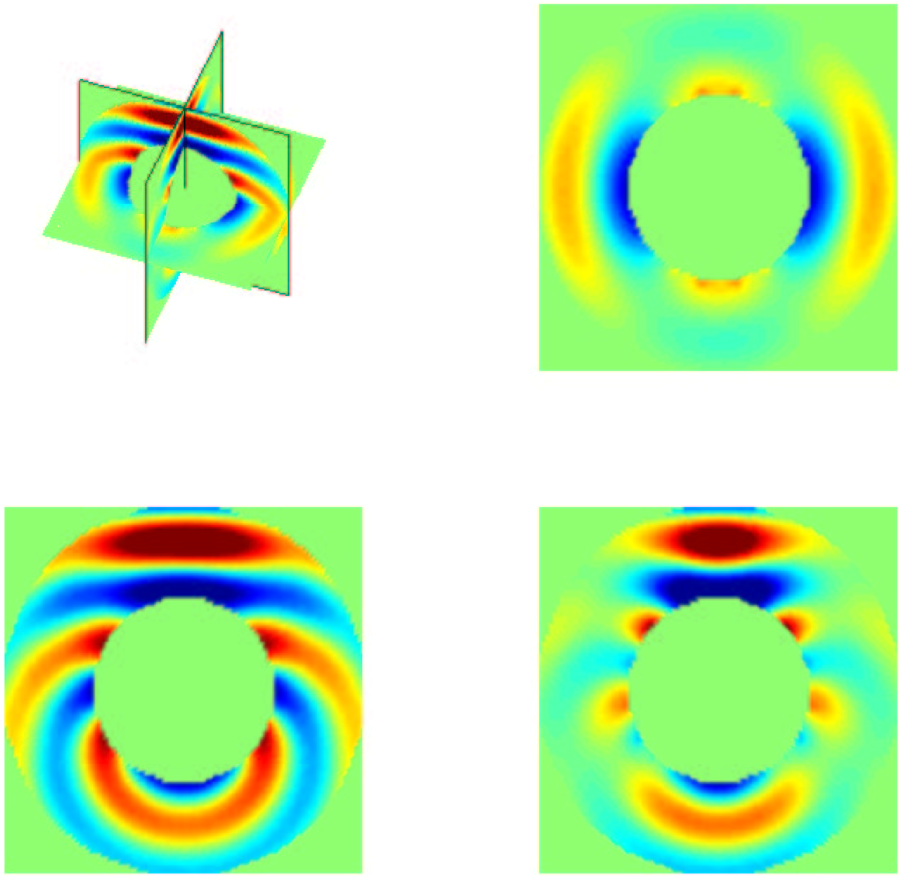

Real part of the diffracted field E_x

Numerical results

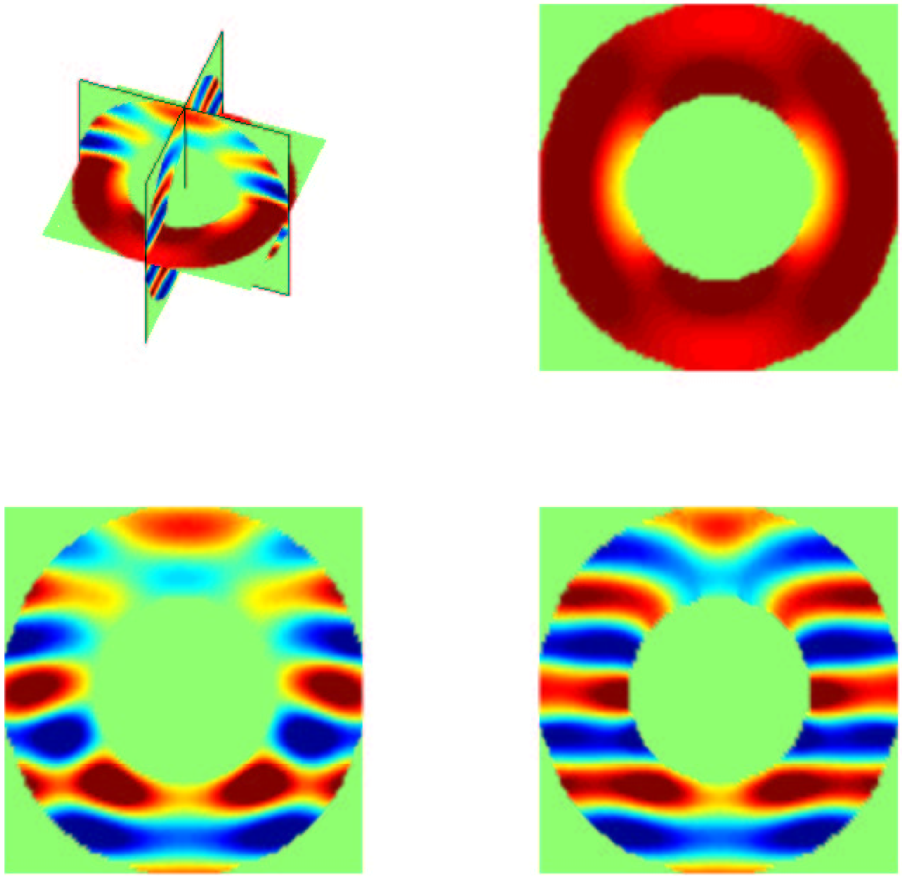

Real part of the total field E_x

Future work

- Systematic study in 3-D case
- Look for preconditioning techniques
- Eigenvalue problem